

Two Different Role Division Control Strategies for Torque and Axial Force of Conical Bearingless Switched Reluctance Motor

HAO Zhenyang*, MIAO Wei, CAO Xin, ZHANG Qiyao

College of Automation Engineering, Nanjing University of Aeronautics and Astronautics, Nanjing 211106, P. R. China

(Received 10 August 2020; revised 23 October 2020; accepted 17 December 2020)

Abstract: Although the five-degree-of-freedom magnetic levitation system composed of two conical bearingless switched reluctance motors (CBSRMs) owns the simplest structure, the torque and levitation forces are coupled greatly. Therefore, it is difficult to make the rotor rotate and be fully levitated simultaneously. To solve this problem, two different role division control strategies are proposed in this paper, i.e. individual role division and mutual role division control strategies. The difference between them is the selection of motor which controls the torque or the axial force. In order to understand the characteristics of control variables, the principle and mathematical model of CBSRM are introduced. After that, two control strategies are explained in detail. To verify the demonstrated performance, the simulations are completed with MATLAB/Simulink.

Key words: five-degree-of-freedom magnetic levitation; conical bearingless switched reluctance motor (CBSRM); individual role division control; mutual role division control

CLC number: TM352

Document code: A

Article ID: 1005-1120(2020)06-0848-10

0 Introduction

In high-speed drive systems, the bearings of motors must satisfy the essential requirements, awesome lubrication and high reliability. Therefore, magnetic bearings are more popular than mechanical bearings in which the rotor can be levitated by controlling winding currents of bearings actively. Due to the particular axial space for the installation of magnetic bearings, the axial length of whole magnetic levitation drive system is increased, which leads to the decrease of the rotor critical speed^[1-2]. Therefore, bearingless motors were proposed and developed to shorten the axial length of five-degree-of-freedom (DOF) magnetic levitation drive system, which integrates the levitation functions into conventional motors. Bearingless switched reluctance motor (BSRM) inherits the robust structure, easy control and high-speed capability from conventional switched reluctance motor (SRM)^[3-5]. To

construct a 5-DOF magnetic levitation system with BSRMs, two BSRMs and one axial magnetic bearing are required, because one BSRM can only generate 2-DOF radial levitation. Therefore, to remove the axial magnetic bearing to further shorten the axial length, the concept of conical bearingless motors was proposed firstly in permanent magnetic synchronous motors^[6-9].

This paper focuses on the conical bearingless switched reluctance motor (CBSRM). The 5-DOF magnetic levitation system made up of two 6/4 CBSRMs is the simplest structure. The decrease of windings reduces the volume of the asymmetrical half-bridge converters. These advantages bring out the challenge of control. There are many variables need to control, and the couplings among them are intensive in this nonlinear system. It is necessary to realize the coordinate control of torque, radial levitation and axial levitation. Firstly, these strategies take advantage of equivalent transformation between

*Corresponding author, E-mail address: zhenyang_hao@nuaa.edu.cn.

How to cite this article: HAO Zhenyang, MIAO Wei, CAO Xin, et al. Two different role division control strategies for torque and axial force of conical bearingless switched reluctance motor[J]. Transactions of Nanjing University of Aeronautics and Astronautics, 2020, 37(6): 848-857.

<http://dx.doi.org/10.16356/j.1005-1120.2020.06.003>

single-winding and dual-winding^[10]. Current of each winding is constructed as torque current, axial-force current and radial-force current in Ref.[11]. Torque current is responsible for the angular velocity, axial-force current for axial position, while radial-force current for radial position. According to the difference of construction, the single machine control and flexible control strategies are proposed^[12-13]. All these strategies conduct two phases, and torque current and axial-force current are components of the same winding current. Therefore, the interaction between torque and axial force control is strong. Li et al.^[14] proposed a compensation control method which conducted the third phase to compensate the axial force of system. However, the energization of the third phase would produce negative torque.

This paper proposes two different role division control strategies for torque and axial force. With regard to the single CBSRM, the winding currents are divided into bias current and radial-force current. Only one of the torque and axial force can be controlled by regulating the bias current. Therefore, the system consists of two CBSRMs, if one controls the system torque, the other must be in charge of the system axial force. The individual role division control strategy (Strategy I) fixes the responsibility of two motors. Moreover, the mutual role division control strategy (Strategy II) keeps on changing the role of each motor according to the actual work condition. The influence between torque and axial force is weaker than other methods that are mentioned above.

1 Principle of CBSRM

Compared with the BSRM, the stator and rotor of the CBSRM are both in the shape of cone. As shown in Fig.1, there is only one set of windings

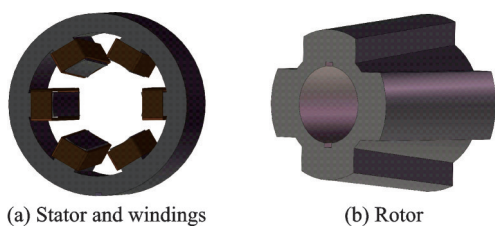


Fig.1 Structure of CBSRM

mounted on each stator pole, whose current is controlled independently. Two CBSRMs are installed as shown in Fig.2, thus constructing the 5-DOF suspension system. According to the arrangement of two motors, the directions of axial force are opposite.

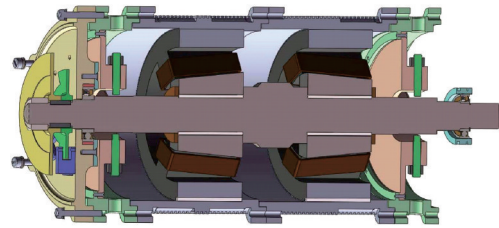


Fig.2 Structure of 5-DOF suspension system

The magnetic pull F will be produced if the winding is energised. Taking phase A as example, the magnetic pull F is distributed in three-dimension owing to the conical air gap. F can be divided into an axial force F_z and a cross-sectional force F_{cs} , as shown in Fig.3(a). Moreover, F_{cs} can be decomposed into a radial force F_r and a tangential force F_t , as shown in Fig.3(b), where A_1 is one winding of phase A. The rotor can be levitated by F_r and rotate with the force F_t . The axial forces of two motors are in opposite direction, and the axial position can be controlled by regulating two axial forces F_{1z} and F_{2z} .

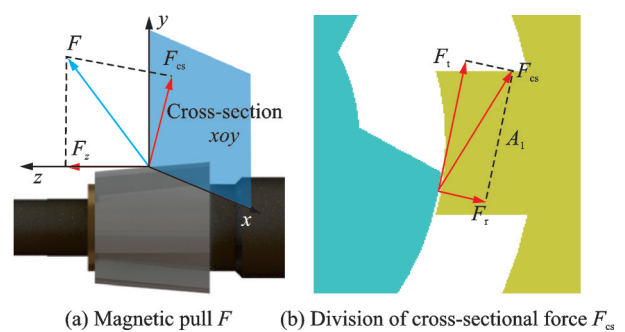


Fig.3 Decomposition of magnetic pull

2 Mathematical Model of CBSRM

In 6/4 CBSRM, there are three phases which own two windings independently. The distribution of windings is presented in Fig.4, where A_1 , A_2 , B_1 , B_2 , C_1 and C_2 are windings of phases A, B and C, respectively, and λ and σ the angles between the rotating coordinate system and the Cartesian coordinate system. To ensure radial force in any direction,

two phases need to be energised at the same time. The order of energization is related to profile of inductance. For SRM, the negative torque will be produced if the phase whose inductance profile possesses negative slope is conducted. The self-inductance profiles of three phases L_{a1} , L_{b1} , L_{c1} are presented in Fig. 5. Two phases of CBSRM are energized each time, in the order of phases AB, CA, BC circularly.

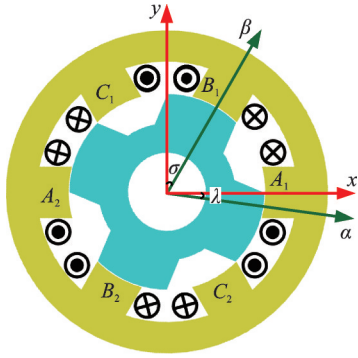


Fig. 4 Distribution of windings in CBSRM

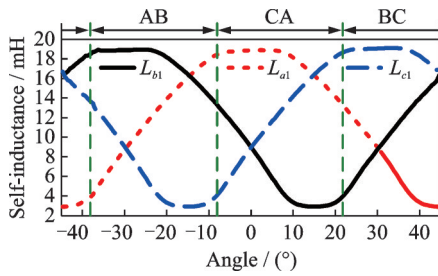


Fig. 5 Inductance profile of CBSRM

Ref. [15] deduced the mathematical model in rotating coordinate system with the method of virtual displacement. Taking phases A and B energised as an example, the torque and levitation forces can be expressed as follows

$$F_a = K_{f1}(i_{a1}^2 - i_{a2}^2) + K_{f2}(i_{a1} + i_{a2})(i_{b1} - i_{b2}) \quad (1)$$

$$F_\beta = K_{f3}(i_{b1}^2 - i_{b2}^2) + K_{f4}(i_{a1} - i_{a2})(i_{b1} + i_{b2}) \quad (2)$$

$$F_z = K_{f5}(i_{a1}^2 + i_{a2}^2) + K_{f6}i_{b1}i_{b2} + K_{f7}(i_{b1}^2 + i_{b2}^2) + K_{f8}i_{a1}i_{a2} + K_{f9}(i_{a1} - i_{a2})(i_{b1} - i_{b2}) \quad (3)$$

$$T = J_1(i_{a1}^2 + i_{a2}^2) + J_2(i_{b1}^2 + i_{b2}^2) + J_3(i_{a1} - i_{a2})(i_{b1} - i_{b2}) + J_4i_{a1}i_{a2} + J_5i_{b1}i_{b2} \quad (4)$$

$$F_z = (M_1 + M_2)i_m^2 + \frac{1}{i_m^2 D^2} [M_3(A_1 F_x - A_2 F_y)^2 + M_4(A_4 F_y - A_3 F_x)^2 + M_5(A_1 F_x - A_2 F_y)(A_4 F_y - A_3 F_x)] \quad (15)$$

$$T = (N_1 + N_2)i_m^2 + \frac{1}{i_m^2 D^2} [N_3(A_1 F_x - A_2 F_y)^2 + N_4(A_4 F_y - A_3 F_x)^2 + N_5(A_1 F_x - A_2 F_y)(A_4 F_y - A_3 F_x)] \quad (16)$$

$$F_x = F_a \cos \sigma + F_\beta \sin \lambda \quad (5)$$

$$F_y = F_\beta \cos \lambda - F_a \sin \sigma \quad (6)$$

where F_a and F_β are radial forces in the rotating coordinate system, and F_x and F_y the radial forces in the Cartesian coordinate system. T is the torque and F_z the axial force of one motor. i_{a1} , i_{a2} , i_{b1} , i_{b2} are the currents of winding A_1 , A_2 , B_1 , B_2 , respectively. K_{f1} — K_{f9} are the coefficients of levitation forces and J_1 — J_5 are the ratios of torque.

To simplify the model derived above, the phase currents are decomposed based on the equivalent transformation between dual-winding and single-winding currents. The expressions of currents are presented as follows

$$i_{a1} = i_{m1} + i_{t1} \quad (7)$$

$$i_{a2} = i_{m1} - i_{t1} \quad (8)$$

$$i_{b1} = i_{m2} + i_{t2} \quad (9)$$

$$i_{b2} = i_{m2} - i_{t2} \quad (10)$$

where i_{m1} and i_{m2} are bias currents of winding A_1 , A_2 , B_1 , B_2 . i_{t1} is the radial-force current of phase A and i_{t2} regulates the radial force of phase B.

Eqs.(1)—(6) can be rewritten as

$$F_x = R_1 i_{m1} i_{t1} + R_2 i_{m2} i_{t1} + R_3 i_{m1} i_{t2} + R_4 i_{m2} i_{t2} \quad (11)$$

$$F_y = S_1 i_{m1} i_{t1} + S_2 i_{m2} i_{t1} + S_3 i_{m1} i_{t2} + S_4 i_{m2} i_{t2} \quad (12)$$

$$F_z = M_1 i_{m1}^2 + M_2 i_{m2}^2 + M_3 i_{t1}^2 + M_4 i_{t2}^2 + M_5 i_{t1} i_{t2} \quad (13)$$

$$T = N_1 i_{m1}^2 + N_2 i_{m2}^2 + N_3 i_{t1}^2 + N_4 i_{t2}^2 + N_5 i_{t1} i_{t2} \quad (14)$$

where R_1 — R_4 , S_1 — S_4 are coefficients of radial levitation forces, M_1 — M_5 related to axial levitation forces, and N_1 — N_5 decide the torque at different angles.

3 Different Role Division Control Strategies of CBSRMs

3.1 Control analysis of CBSRM

In order to improve tracking performance of currents during commutation, i_{m1} usually equals i_{m2} . If $i_{m1} = i_{m2} = i_m$, Eqs.(13) and (14) can be transformed into

where $A_1 = S_3 + S_4$, $A_2 = R_3 + R_4$, $A_3 = S_1 + S_2$, $A_4 = R_1 + R_2$, $D = A_1 A_4 - A_2 A_3$. When the rotor is fully levitated, the average levitation forces F_x and F_y are constant. According to Eqs.(15) and (16), i_m is the unique variable to control F_z and T . For the single CBSRM, the torque T is regulated by i_m , so the axial force F_z remains to be free.

3.2 Individual role division control strategy of CBSRMs

The control targets of 5-DOF magnetic suspension system are the rotation and 5-DOF levitation of rotor. There are two motors in the whole system, called CBSRM1# and CBSRM2#. On the basis of characteristics of control variables, the bias current of CBSRM1# i_{1m} is selected to control the torque and the bias current of CBSRM2# i_{2m} is responsible for the axial force of system in a control period. The uncontrolled torque or axial force of each motor can be compensated by each other in the next period.

Owing to the opposite directions, the total axial force of the system F_z is the difference between the absolute value of axial force of CBSRM1# F_{1z} and CBSRM2# F_{2z}

$$F_z = |F_{1z}| - |F_{2z}| \quad (17)$$

In two adjacent control periods, the k th and $(k+1)$ th periods, the axial force of CBSRM1# F_{1z} is considered to be constant.

$$F_{1z(k+1)} = F_{1z(k)} \quad (18)$$

Therefore, the given axial force $F_{z_{ref}(k+1)}$ can be represented as

$$F_{z_{ref}(k+1)} = |F_{1z(k+1)}| - |F_{2z(k+1)}| = |F_{1z(k)}| - |F_{2z(k+1)}| \quad (19)$$

where $F_{z_{ref}(k+1)}$ is obtained by the PID regulator in axial position close-loop, the axial force of CBSRM1# F_{1z} can be observed, and the needed axial force $F_{2z(k+1)}$ is calculated as follows

$$|F_{2z(k+1)}| = |F_{1z(k)}| - F_{z_{ref}(k+1)} \quad (20)$$

Moreover, the bias current of CBSRM2# in the $(k+1)$ th period can be acquired according to Eq.(21).

$$i_{2m(k+1)} = \frac{\sqrt{F_{2z(k+1)} - M_{3(k)} i_{2r1(k)}^2 - M_{4(k)} i_{2r2(k)}^2 - M_{5(k)} i_{2r1(k)} i_{2r2(k)}}}{M_{1(k+1)} + M_{2(k+1)}} \quad (21)$$

where $M_{3(k)} - M_{5(k)}$ are coefficients of axial force in the k th period, while $M_{1(k+1)} - M_{2(k+1)}$ are in the $(k+1)$ th period, and $i_{2r1(k)}$ and $i_{2r2(k)}$ are radial-force currents of CBSRM2# in the k th period.

If the radial force load is light, the torque that radial-force currents produce can be ignored. Then the torque of whole system can be written approximately as

$$T = T_1 + T_2 \approx (N_1 + N_2)(i_{1m}^2 + i_{2m}^2) \quad (22)$$

The current that regulates the torque i_n is obtained by the PI controller of speed close-loop. The bias current of CBSRM2# i_{2m} can be considered to be constant in two control periods due to the free torque of CBSRM2#.

$$i_{2m(k+1)} = i_{2m(k)} \quad (23)$$

So the bias current of CBSRM1# is calculated as follows

$$i_{1m(k+1)} = \sqrt{i_n^2(k+1) - i_{2m(k+1)}^2} = \sqrt{i_n^2(k+1) - i_{2m(k)}^2} \quad (24)$$

The accurate calculation of i_{1m} ensures the compensation of free torque that CBSRM2# produces so as to regulate the torque of system. After the currents i_{1m} , i_{2m} are known, the radial-force currents can be derived according to Eqs.(25)–(28).

$$i_{1r1} = \frac{(S_3 + S_4)F_{1x} - (R_3 + R_4)F_{1y}}{i_{1m}[(R_1 + R_2)(S_3 + S_4) - (S_1 + S_2)(R_3 + R_4)]} \quad (25)$$

$$i_{1r2} = \frac{(S_1 + S_2)F_{1x} - (R_1 + R_2)F_{1y}}{i_{1m}[(R_3 + R_4)(S_1 + S_2) - (S_3 + S_4)(R_1 + R_2)]} \quad (26)$$

$$i_{2r1} = \frac{(S_3 + S_4)F_{2x} - (R_3 + R_4)F_{2y}}{i_{2m}[(R_1 + R_2)(S_3 + S_4) - (S_1 + S_2)(R_3 + R_4)]} \quad (27)$$

$$i_{2r2} = \frac{(S_1 + S_2)F_{2x} - (R_1 + R_2)F_{2y}}{i_{2m}[(R_3 + R_4)(S_1 + S_2) - (S_3 + S_4)(R_1 + R_2)]} \quad (28)$$

3.3 Mutual role division control strategy of CBSRMs

The roles of each motor in the control strategy mentioned above are arranged. Similarly, two motors can exchange its role, thus introducing another control strategy. When the roles of each motor can change as the need of situation, the strategy is named mutual role division control. As shown in Table 1, there are two arranged role division ways. The bias currents of two motors in the first way

can be obtained by Eqs. (29) — (30), while currents in the second way can be obtained by

$$i_{2m(k+1)} = \sqrt{\frac{-|F_{1z(k+1)}| + F_{z_{ref}(k+1)} - M_{3(k+1)}i_{2l1(k+1)}^2 - M_{4(k+1)}i_{2l2(k+1)}^2 - M_{5(k+1)}i_{2l1(k+1)}i_{2l2(k+1)}}{M_{1(k+1)} + M_{2(k+1)}}} \quad (30)$$

$$i_{2m(k+1)} = \sqrt{i_{n(k+1)}^2 - i_{1m(k+1)}^2} \quad (31)$$

$$i_{1m(k+1)} = \sqrt{\frac{-|F_{2z(k+1)}| - F_{z_{ref}(k+1)} - M_{3(k+1)}i_{1l1(k+1)}^2 - M_{4(k+1)}i_{1l2(k+1)}^2 - M_{5(k+1)}i_{1l1(k+1)}i_{1l2(k+1)}}{M_{1(k+1)} + M_{2(k+1)}}} \quad (32)$$

Table 1 Two arranged role division ways

Arranged role division way	Motor controlling torque	Motor controlling axial force
The first way	CBSRM1#	CBSRM2#
The second way	CBSRM2#	CBSRM1#

The principle to evaluate which way to choose is called the cost-function. The cost-function in mutual role division control is shown as

$$f = k_1(i_{1m(k+1)} - i_{1m(k)})^2 + k_2(i_{2m(k+1)} - i_{2m(k)})^2 \quad (33)$$

where k_1 and k_2 are weight coefficients, which decide the proportion of torque and axial force in cost-function. According to the values of cost-function in two ways, the smaller would be preferred. The flow chart of mutual role division control strategy is shown in Fig.6.

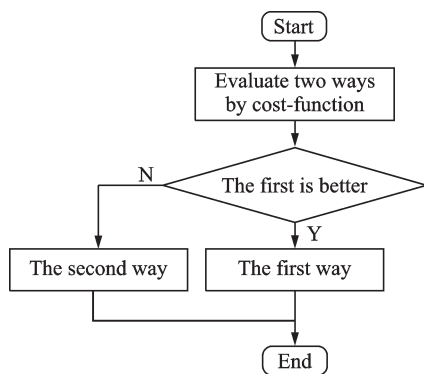


Fig.6 Flow chart of mutual role division control strategy

3.4 Comparison of two different role division control strategies

The contents above have detailed analysis of two strategies. Obviously, the mutual role division control is an improvement of individual role division control. The roles of two motors are flexible according to the working conditions. Therefore, the applications of mutual role division have broadened. For example, in the circumstance of higher require-

Eqs.(31)—(32).

$$i_{1m(k+1)} = \sqrt{i_{n(k+1)}^2 - i_{2m(k+1)}^2} \quad (29)$$

ments for torque control accuracy, the mutual control is more flexible to regulate weight coefficients, so as to improve the dynamic and steady-state performance of torque current tracking. However, complication of calculation and control comes with flexibility of role adjustment.

4 Simulation Results

4.1 Parameters of simulation

To verify the theory analysis, simulations of two strategies are carried out in MATLAB/Simulink. The parameters of simulation are shown in Table 2.

Table 2 Parameters of simulation

Parameter	Value
Outer diameter of stator/mm	115
Outer diameter of small end of rotor/mm	48.7
Height of stator yoke/mm	11.14
Height of rotor tooth/mm	6.75
Diameter of shaft/mm	25
Axial cone angle of stator and rotor/(°)	6
Winding turns	84
Average air gap length of stator and rotor/mm	0.25
Lamination length of core/mm	50
Average air gap length of auxiliary bearing at suspension end/mm	0.1
Bus voltage/V	180
Reference of speed/(r·min ⁻¹)	1 000—1 500@3 s
Load torque/(mN·m)	80
Reference of axial force/N	-20—20@1.5 s
Reference of radial force in <i>x</i> direction of CBSRM1#/N	10
Reference of radial force in <i>y</i> direction of CBSRM1#/N	15
Reference of radial force in <i>x</i> direction of CBSRM2#/N	9
Reference of radial force in <i>y</i> direction of CBSRM2#/N	16

4.2 Simulation results of individual role division control strategy

Fig.7 shows the waveforms of speed and torque. When the speed reference changes suddenly at 3 s, the speed of motor can trace the reference from 1 000 r/min to 1 500 r/min very well. According to Fig.7 (b), the torque of CBSRM2# also increases even though the torque of CBSRM2# is free. The reason is that the torque of CBSRM1# increases in order to raise the speed, then the axial force of CBSRM1# is bigger, thus the bias current of CBSRM2# that compensates axial force of CBSRM1# increases. Eventually, the torque of CBSRM2# turns to be larger.

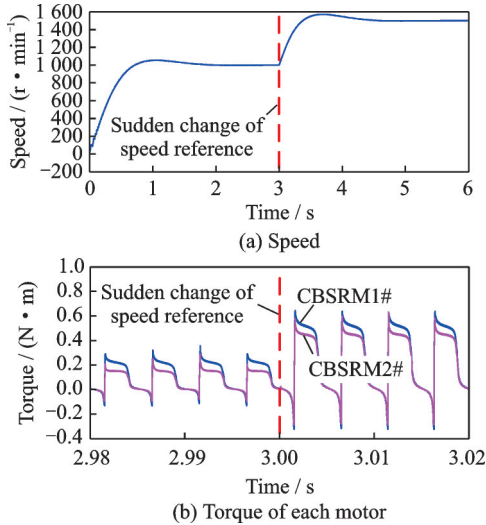


Fig.7 Simulation results of speed and torque during the change of speed reference using Strategy I

The sudden change of axial force reference occurs at 1.5 s, as shown in Fig.8, and the axial force can always trace the reference even if the reference changes from -20 N to 20 N at 1.5 s. And the bias current of CBSRM2# is regulated to compensate the axial force as the reference changes.

The waveforms of torque during the sudden change of axial force are shown in Fig.9, while the waveforms of axial force when the increase of speed occurs are shown in Fig.10. When the axial force reference increases at 1.5 s, the axial force of CBSRM2# F_{z_c} must decrease, and the torque of CBSRM2# also decreases with the bias current i_{2m} . Owing to the compensation torque of CBSRM1#, the total torque T keeps constant. Similarly, with the

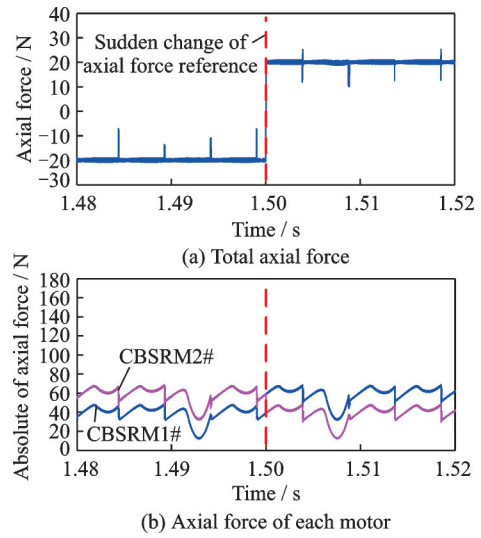


Fig.8 Simulation results of axial force during the change of axial force reference using Strategy I

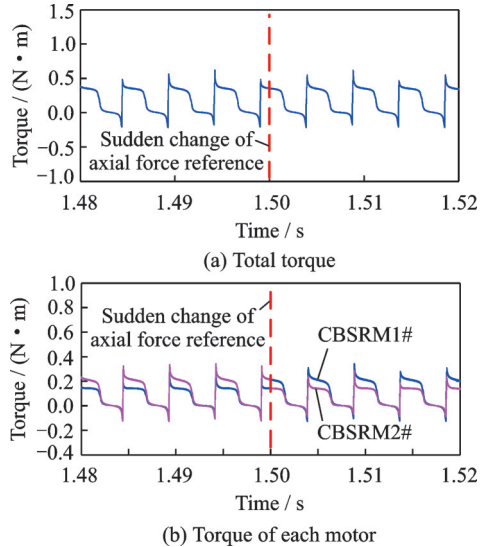


Fig.9 Simulation results of torque during the sudden change of axial force reference using Strategy I

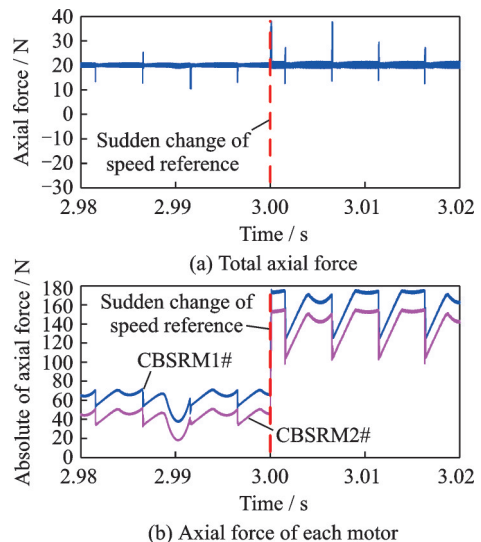


Fig.10 Simulation results of axial force during the sudden change of speed reference using Strategy I

compensation axial force of CBSRM2#, the total axial force is not affected by the increase of speed.

According to Fig.11, the radial forces all trace its reference respectively. However, the force waveform in Fig.11 has burred feature which appears at the commutation of phases.

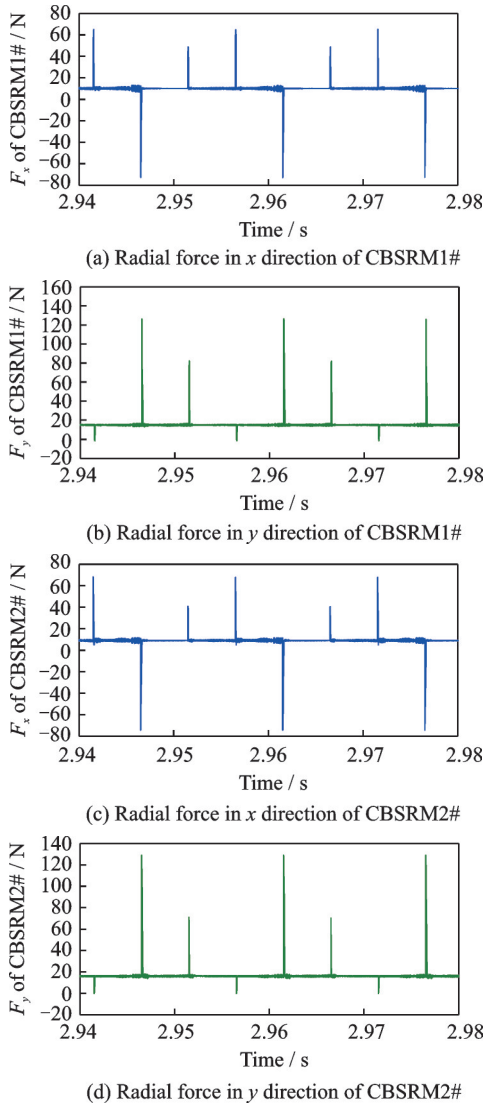


Fig.11 Simulation results of radial forces using Strategy I

This is due to the winding currents adopt hysteresis control. The reference of winding current changes suddenly but the real current cannot react immediately at commutation. Meanwhile, the mathematical model of CBSRM is derived in different sections. The force is calculated by the expression which consists of winding currents. Therefore, the control strategy can realize the speed regulation and 5-DOF levitation of rotor simultaneously, with excellent dynamic and steady-state performance.

4.3 Simulation results of mutual role division control strategy

The simulation parameters of mutual role division are as same as those of individual role division control strategy. Furthermore, in the cost-function k_1 equals k_2 . The simulation results of mutual role division validate the correctness of theory. The waveforms of speed and torque during the sudden change of speed reference are shown in Fig.12. The speed of motors can track the reference quickly and accurately. And the torques of two motors both grow with the increase of speed.

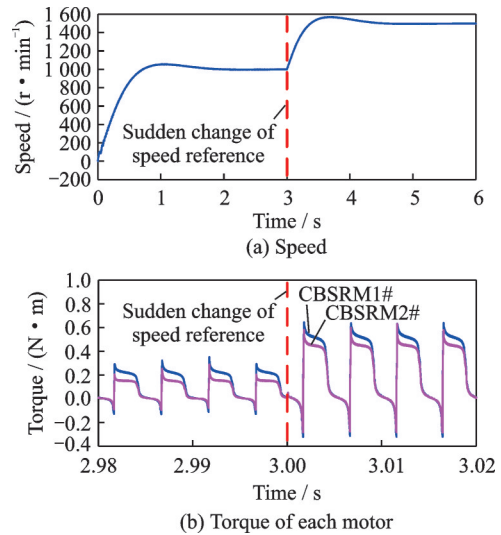


Fig.12 Simulation results of speed and torque during the change of speed reference using Strategy II

As shown in Fig.13, the axial forces of two motors cooperate with each other so as to bring the total axial force from -20 N to 20 N rapidly. To show the switches between two role division ways, the signal during the change of axial force reference is presented. “1” represents the first way, while “0” the second way. It can be seen from the Fig.14 that two role division ways alternate according to the evaluation principle. Combined with Fig.12(a) and Fig.13(a), the speed and axial force both make efforts to trace the references despite the continuous switches between two ways.

In order to verify the decoupling performance of mutual role division control, the waveforms of torque during the sudden change of axial force at 1.5 s are shown in Fig.15, while waveforms of axial

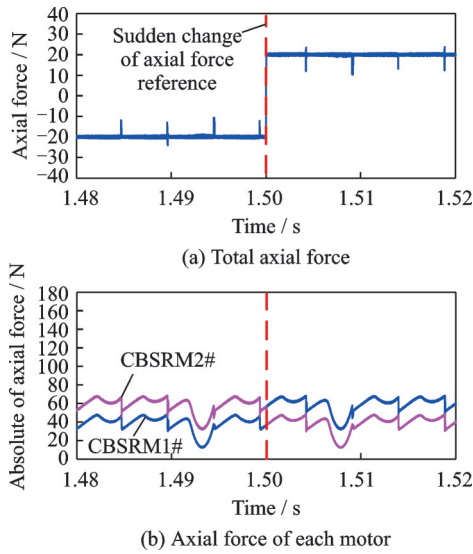


Fig.13 Simulation results of axial force during the change of axial force reference using Strategy II

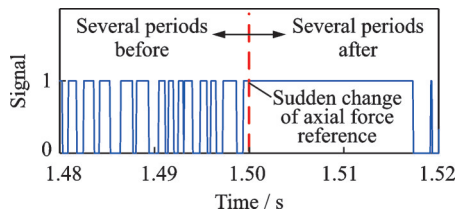


Fig.14 Switches between two role division ways

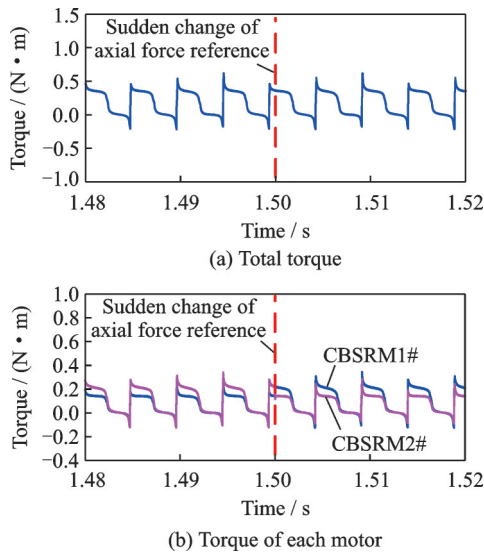


Fig.15 Simulation results of torque during the sudden change of axial force reference using Strategy II

force during the sudden change of speed at 3 s are shown in Fig.16. The total torque and axial force are almost constant. The reasons are similar to those of individual role division control.

The waveforms of radial forces of two motors are given in Fig.17. All of them track their referenc-

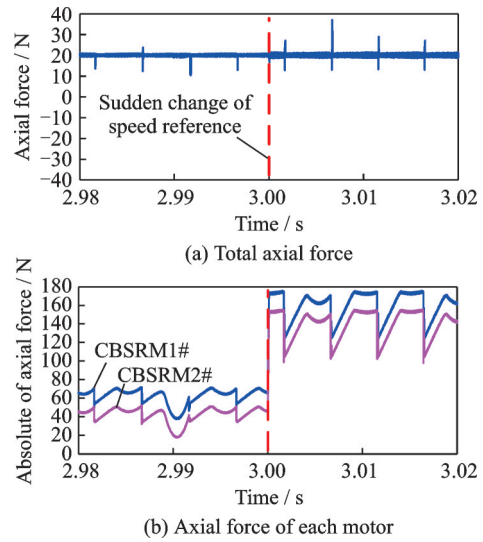


Fig.16 Simulation results of axial force during the sudden change of speed reference using Strategy II

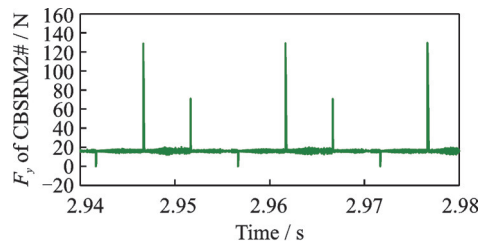
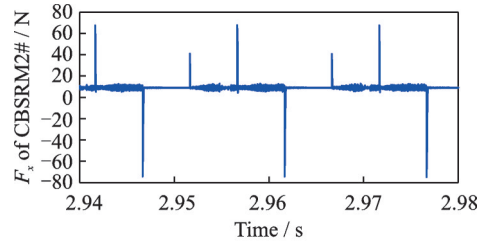
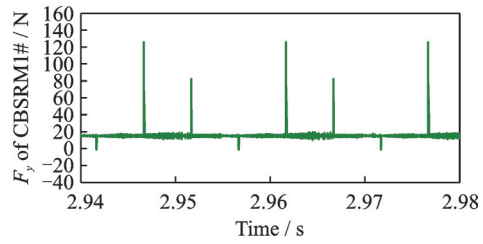
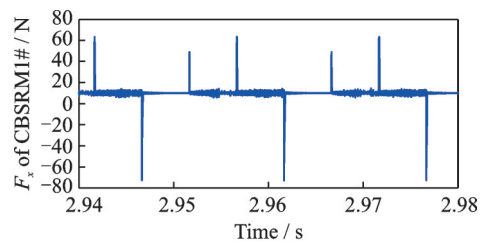


Fig.17 Simulation results of radial forces using Strategy II

es as expectation so as to realize the radial levitation of rotors.

5 Conclusions

This paper proposes two coordinate control strategies of torque and levitation forces of 5-DOF magnetic suspension system which is made up of two CBSRMs. Individual role division control strategy makes two motors take charge of different responsibilities, i. e., one to control torque and the other to control axial force. The roles of two motors are not immutable, and mutual role division control strategy has a more widely application on the basis of individual role division. The coefficients of cost-function can change according to the need of operation, thus deciding the roles of two motors. Two strategies realize the decoupling of torque and axial force by means of control to a certain extent and propose a new solution for the application of the high integrated 5-DOF magnetic levitation system.

References

- [1] FANG J, XU S. Effects of eddy current in electrical connection surface of laminated cores on high-speed PM motor supported by active magnetic bearings[J]. *IEEE Transactions on Magnetics*, 2015, 51(11): 1-4.
- [2] TEZUKA T, KURITA N, ISHIKAWA T. Design and simulation of a five degrees of freedom active control magnetic levitated motor[J]. *IEEE Transactions on Magnetics*, 2013, 49(5): 2257-2262.
- [3] GONG C, LI S, HABETLER T, et al. Direct position control for ultrahigh-speed switched-reluctance machines based on low-cost nonintrusive reflective sensors[J]. *IEEE Transactions on Industry Applications*, 2019, 55(1): 480-489.
- [4] XUE B, WANG H, TANG S, et al. Levitation performance analysis for bearingless switched reluctance motor[C]//*Proceedings of 2015 18th International Conference on Electrical Machines and Systems (ICEMS)*. Pattaya, Thailand:[s.n.], 2015: 264-270.
- [5] CAO Xin, CHEN Huateng, DENG Zhiquan. Analogy study of two types of multi-degree-of-freedom switched reluctance motors[J]. *Journal of Nanjing University of Aeronautics & Astronautics*, 2020, 52(2): 171-180. (in Chinese)
- [6] XU S, FANG J. A novel conical active magnetic bearing with claw structure[J]. *IEEE Transactions on Magnetics*, 2014, 50(5): 1-8.
- [7] KASCAK P, JANSEN R, DEVER T, et al. Motor-ing performance of a conical pole-pair separated bearingless electric machine[C]//*Proceedings of IEEE 2011 Energy Tech*. Cleveland, OH, USA: IEEE, 2011: 1-6.
- [8] KASCAK P, JANSEN R, DEVER T, et al. Levitation performance of two opposed permanent magnet pole-pair separated conical bearingless motors[C]//*Proceedings of 2011 IEEE Energy Conversion Congress and Exposition*. Phoenix, AZ, USA: IEEE, 2011: 1649-1656.
- [9] DEMIR U, ROGGIA S, AKÜNER M C. Comparison between two conical induction machines designed for an electric vehicle application[C]//*Proceedings of 2019 IEEE International Electric Machines & Drives Conference (IEMDC)*. San Diego, CA, USA: IEEE, 2019: 1032-1037.
- [10] CAO X, YANG H, DENG Z, et al. Equivalent transformation and control for single-winding bearingless switched reluctance motors[J]. *Electric Power Components and Systems*, 2016, 44(9): 1040-1050.
- [11] LIU C, CAO X, LI X, et al. Current delta control for conical bearingless switched reluctance motors[C]//*Proceedings of 2018 13th IEEE Conference on Industrial Electronics and Applications (ICIEA)*. Wuhan, China: IEEE, 2018: 2075-2078.
- [12] MIAO W, CAO X, LI X, et al. Single machine control of axial force for conical bearingless switched reluctance motors[C]//*Proceedings of 2019 22nd International Conference on Electrical Machines and Systems (ICEMS)*. Harbin, China:[s.n.], 2019: 1-5.
- [13] CAO X, LI X, DENG Z, et al. A flexible control method of axial force for conical bearingless switched reluctance motors[C]//*Proceedings of 2018 IEEE International Conference on Electrical Systems for Aircraft, Railway, Ship Propulsion and Road Vehicles & International Transportation Electrification Conference (ESARS-ITEC)*. Nottingham, UK: IEEE, 2018: 1-5.
- [14] LI X, CAO X, LIU C, et al. Compensation control of axial force for conical bearingless switched reluctance motors[C]//*Proceedings of 2018 13th IEEE Conference on Industrial Electronics and Applications (ICIEA)*. Wuhan, China: IEEE, 2018: 1886-1891.
- [15] CAO Xin, LI Xiaodi, LIU Chenhao, et al. Mathematical model of conical bearingless switched reluctance motor based on rotating coordinate system[J]. *Transactions of China Electrotechnical Society*, 2018, 33(17): 4029-4036. (in Chinese)

Acknowledgements This work was supported by the National Natural Science Foundations of China (Nos. 51877107, 51577087, 51477074).

Author Dr. HAO Zhenyang received the B.S. and Ph.D. degrees in Electrical Engineering from Nanjing University of Aeronautics and Astronautics (NUAA), Nanjing, China, in 2004 and 2010, respectively. He has been engaged in the teaching and research in the field of Motion Drive from 2010 in NUAA. He has been an associate professor since 2013 in NUAA. His current research interests include permanent magnet motor design, direct torque control and fault tolerant control techniques. He has published over 20 technical papers. He was awarded the scientific and technology achieve-

ment in aeronautics for the project of permanent magnet fault tolerant motor drive system in 2011. He has been PI or Co-PI for over 10 research projects since 2010.

Author contributions Dr. HAO Zhenyang contributed to the background of the study and designed the study. Ms. MIAO Wei compiled the models, conducted the analysis and wrote the manuscript. Prof. CAO Xin revised and modified the manuscript. Ms. ZHANG Qiyao contributed to the data for analysis. All authors commented on the manuscript draft and approved the submission.

Competing interests The authors declare no competing interests.

(Production Editor: ZHANG Huangqun)

适用于锥形无轴承开关磁阻电机转矩和轴向力的两种不同的分工控制方法

郝振洋, 缪伟, 曹鑫, 张绮瑶

(南京航空航天大学自动化学院, 南京 211106, 中国)

摘要:由两台锥形无轴承开关磁阻电机可构成结构最为简单的五自由度磁悬浮系统,但其转矩和悬浮力之间存在较大的耦合,因此很难同时实现转子的旋转和五自由度悬浮。针对这一问题,本文提出了两种不同的分工控制策略,即单分工控制策略和双分工控制策略。二者的区别在于主控转矩电机和主控轴向力电机的选择。为了了解控制变量的特性,介绍了锥形无轴承开关磁阻电机的原理和数学模型,然后详细阐述了两种控制方法。最后,利用MATLAB/Simulink仿真验证了所提算法的性能。

关键词:五自由度磁悬浮;锥形无轴承开关磁阻电机;单分工控制;双分工控制